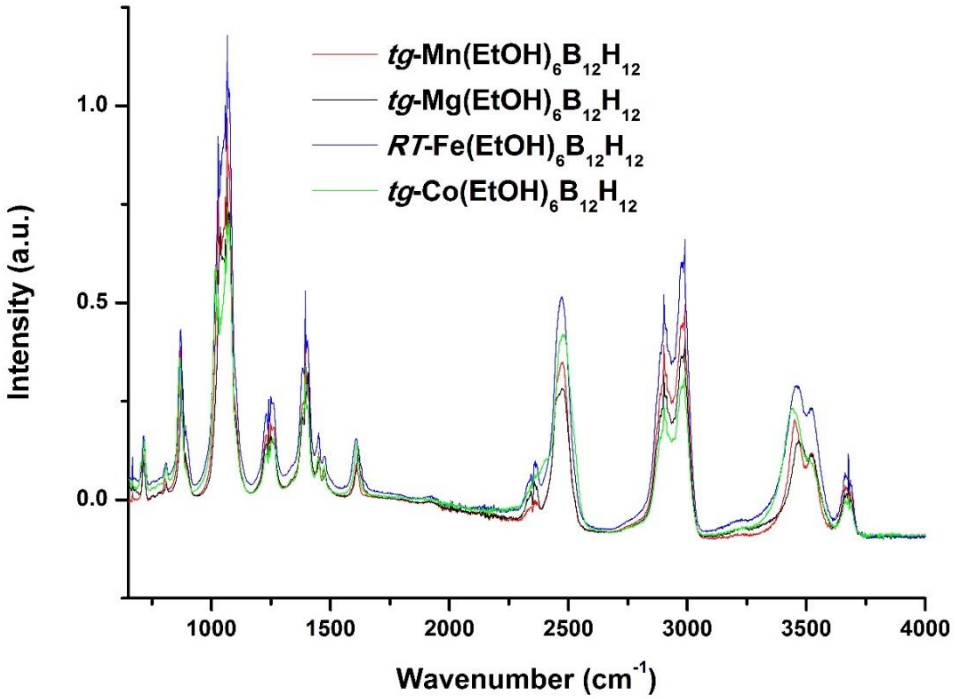

Figure S1. IR spectra of *tg*-Co(EtOH)$_6$B$_{12}$H$_{12}$ (green line), *RT*-Fe(EtOH)$_6$B$_{12}$H$_{12}$ (blue line), *tg*-Mn(EtOH)$_6$B$_{12}$H$_{12}$ (red line) and *tg*-Mg(EtOH)$_6$B$_{12}$H$_{12}$ (black line) at room temperature.

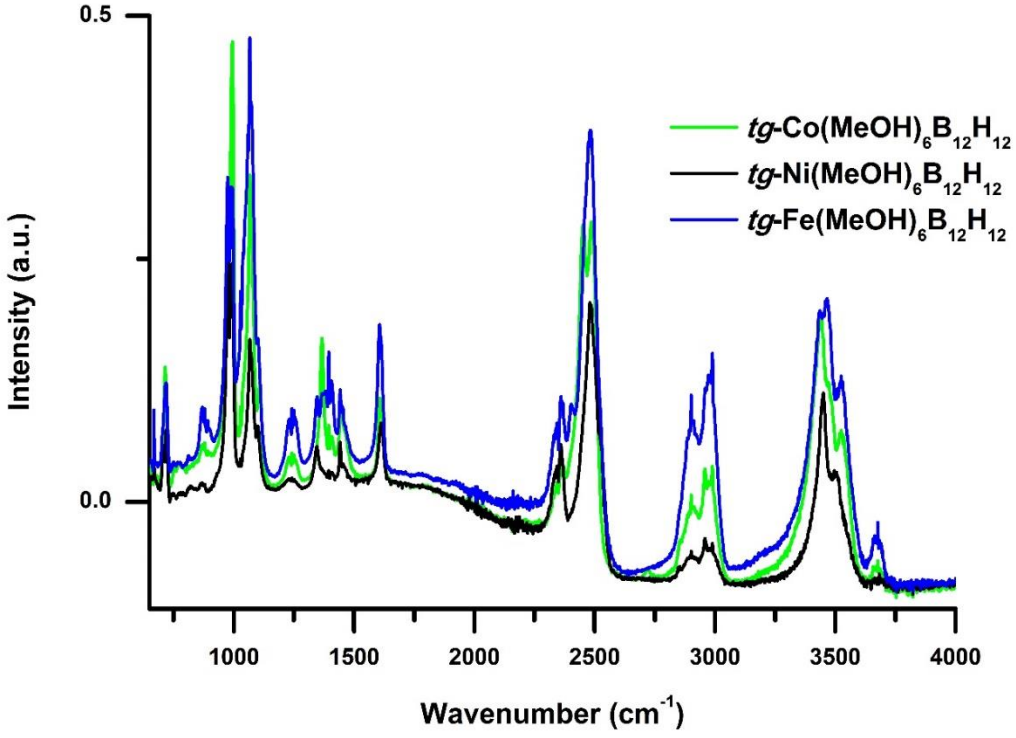

Figure S2. IR spectra of *r*-Co(MeOH)$_6$B$_{12}$H$_{12}$ (green line), *r*-Fe(MeOH)$_6$B$_{12}$H$_{12}$ (blue line) and *r*-Ni(MeOH)$_6$B$_{12}$H$_{12}$ (black line) at room temperature.

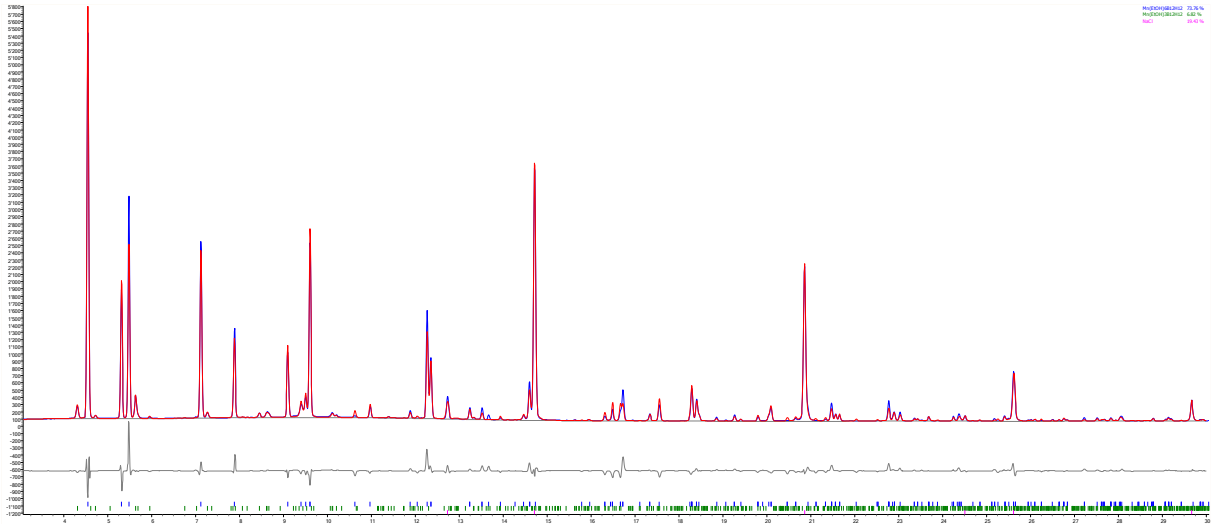

Figure S3. Rietveld plot for refinement of *tg*-$Mn(EtOH)_6B_{12}H_{12}$ at T= 30 °C. SNBL, λ= 0.7225 Å, χ^2 = 3026, R_{wp} (bgr. corrected) = 0.17, R_{Bragg} = 0.08.

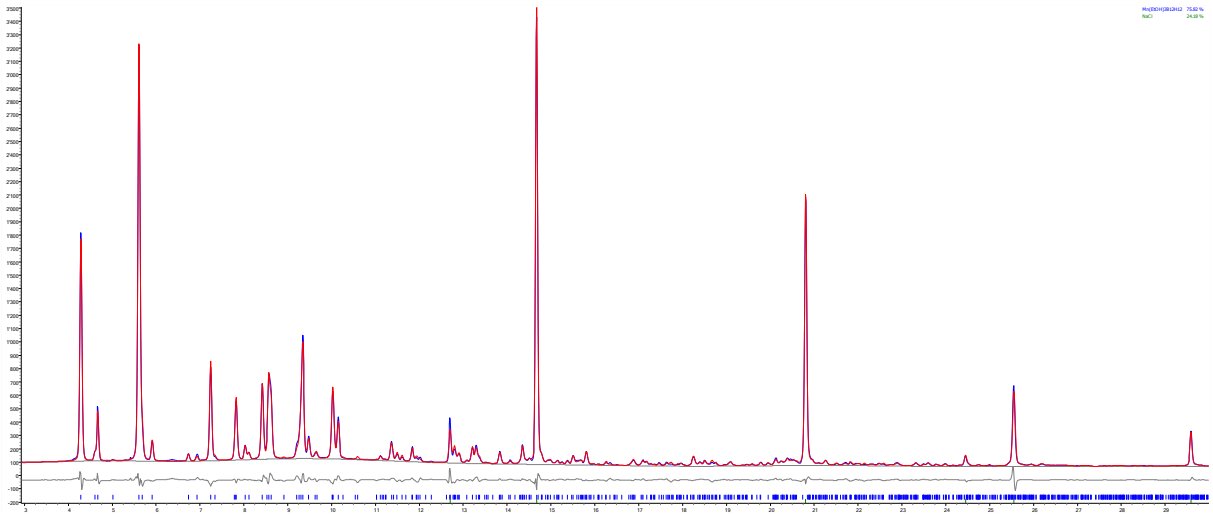

Figure S4. Rietveld plot for refinement of *m*-$Mn(EtOH)_3B_{12}H_{12}$ at T= 109 °C. SNBL, λ= 0.7225 Å, χ^2 = 1303, R_{wp} (bgr. corrected) = 0.09, R_{Bragg} = 0.02.

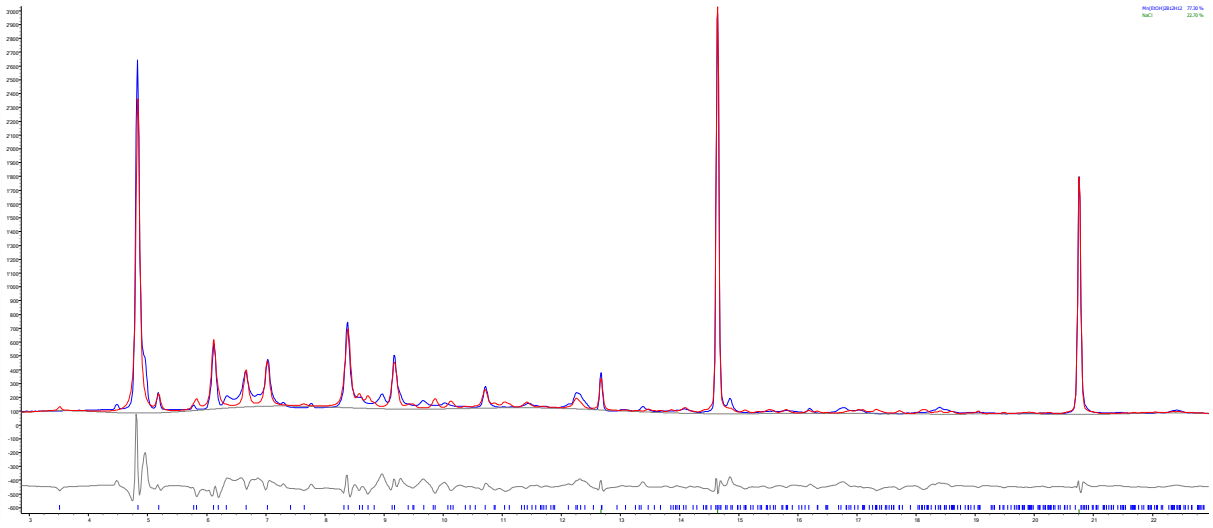

Figure S5. Rietveld plot for refinement of *m*-$Mn(EtOH)_2B_{12}H_{12}$•EtOH at T= 164 °C. SNBL, λ= 0.7225 Å, χ^2 = 3733, R_{wp} (bgr. corrected) = 0.26, R_{Bragg} = 0.08.

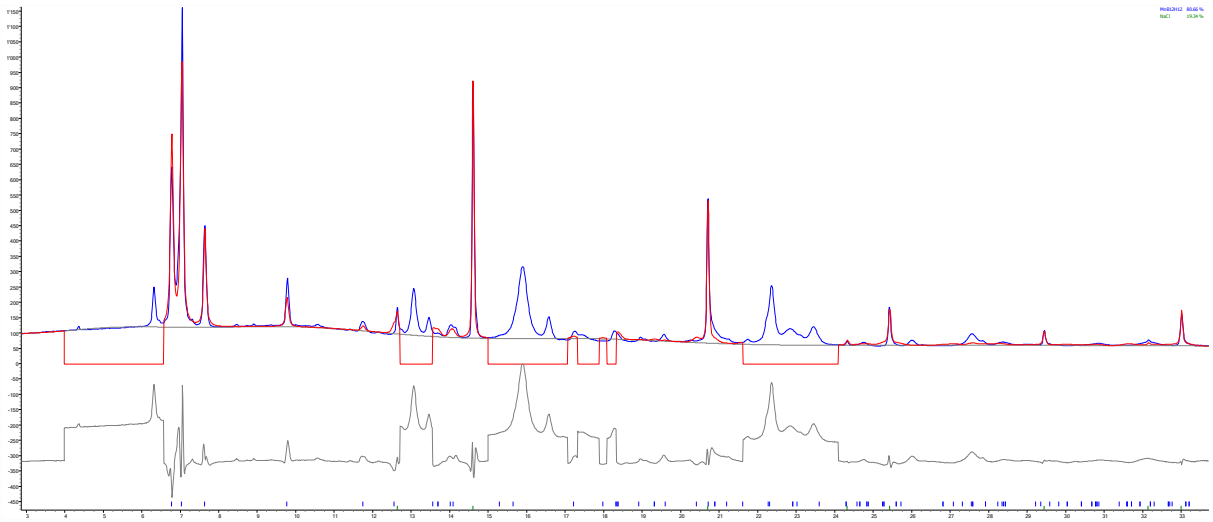

Figure S6. Rietveld plot for refinement of *tg*-$MnB_{12}H_{12}$ at T= 212 °C. SNBL, λ= 0.7225 Å, χ^2 = 3733, R_{wp} (bgr. corrected) = 0.26, R_{Bragg} = 0.08. Peaks of unidentified impurity are excluded.

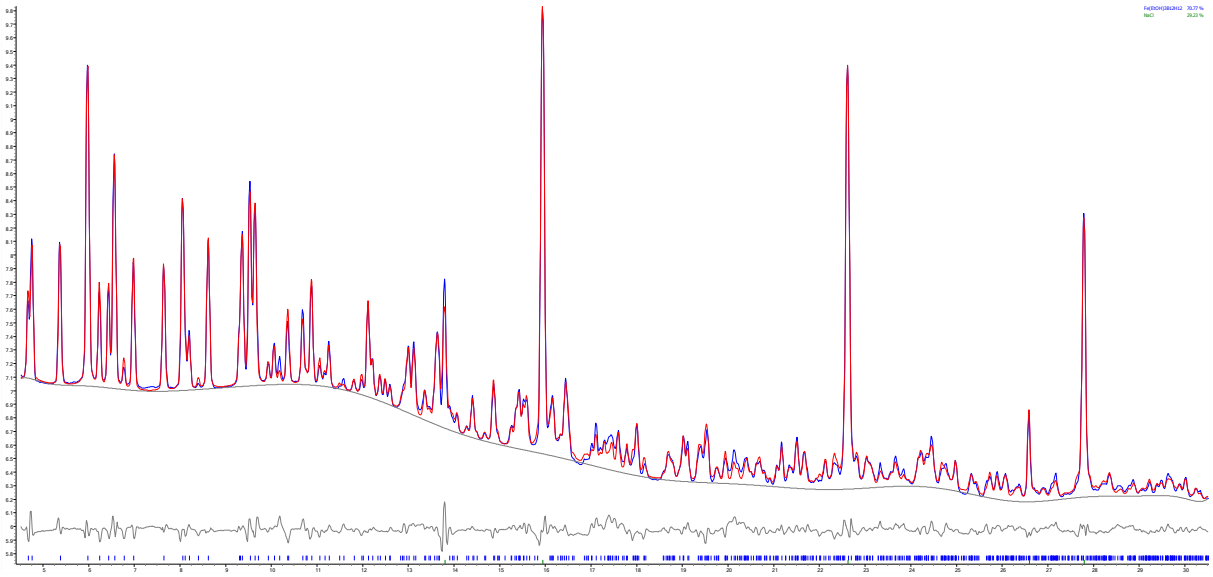

Figure S7. Rietveld plot for refinement of *m*-$Fe(EtOH)_3B_{12}H_{12}$ at T= 109 °C. SNBL, λ= 0.7849 Å, χ^2 = 702, R_{wp} (bgr. corrected) = 0.08, R_{Bragg} = 0.02.

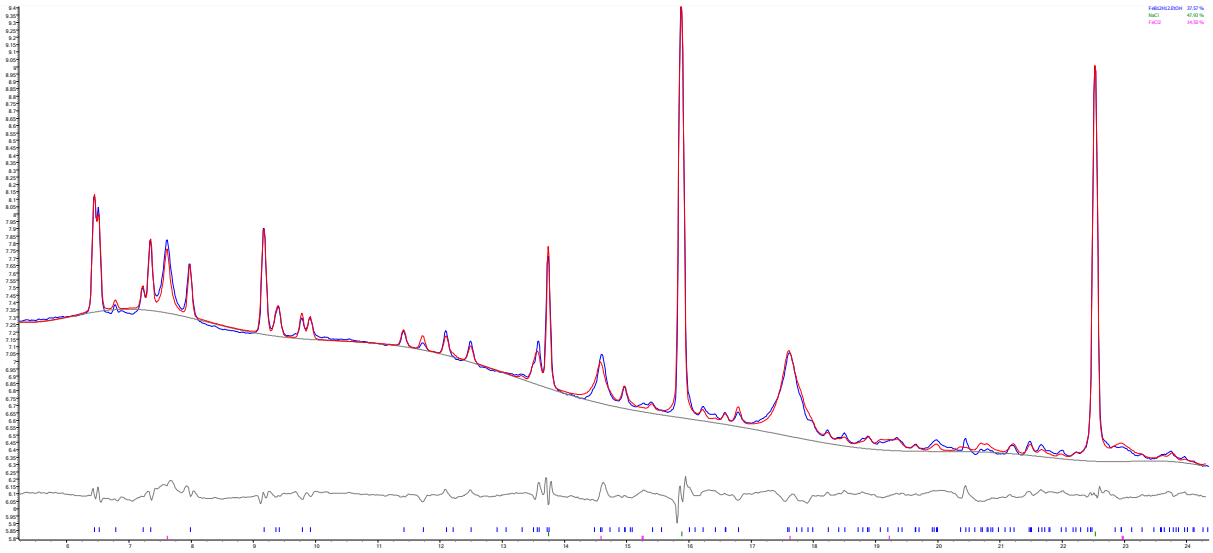

Figure S8. Rietveld plot for refinement of *o*-Fe(EtOH)$B_{12}H_{12}$ at T= 173 °C. SNBL, λ= 0.7849 Å, χ^2 = 484, R_{wp} (bgr. corrected) = 0.09, R_{Bragg} = 0.01.

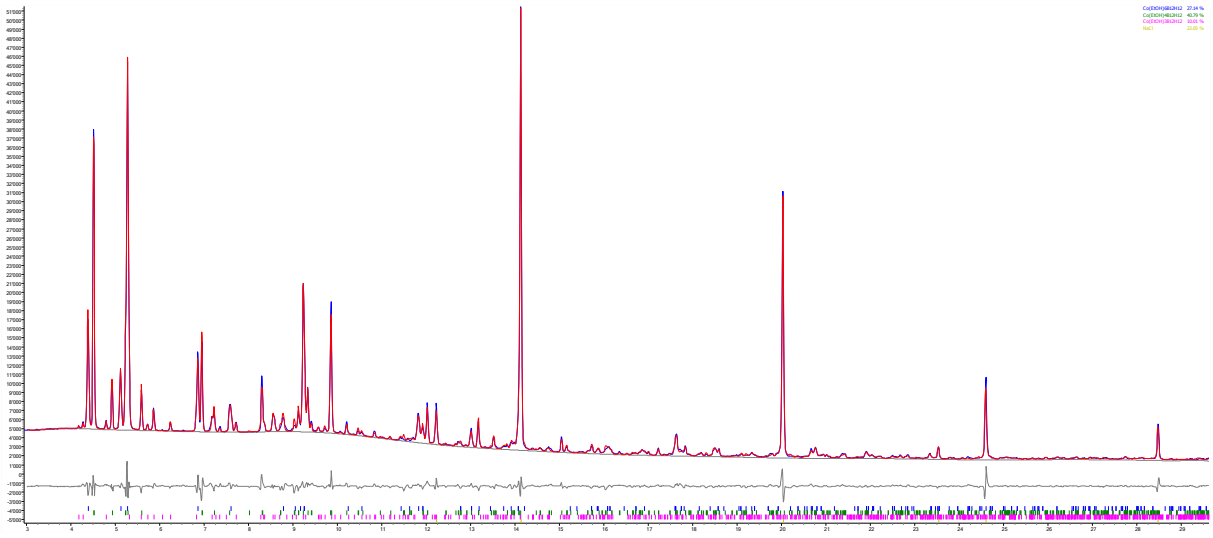

Figure S9. Rietveld plot for refinement of *tg*-Co$(EtOH)_6B_{12}H_{12}$ at T= 40 °C. SNBL, λ= 0.69425 Å, χ^2 = 8910, R_{wp} (bgr. corrected) = 0.11, R_{Bragg} = 0.01.

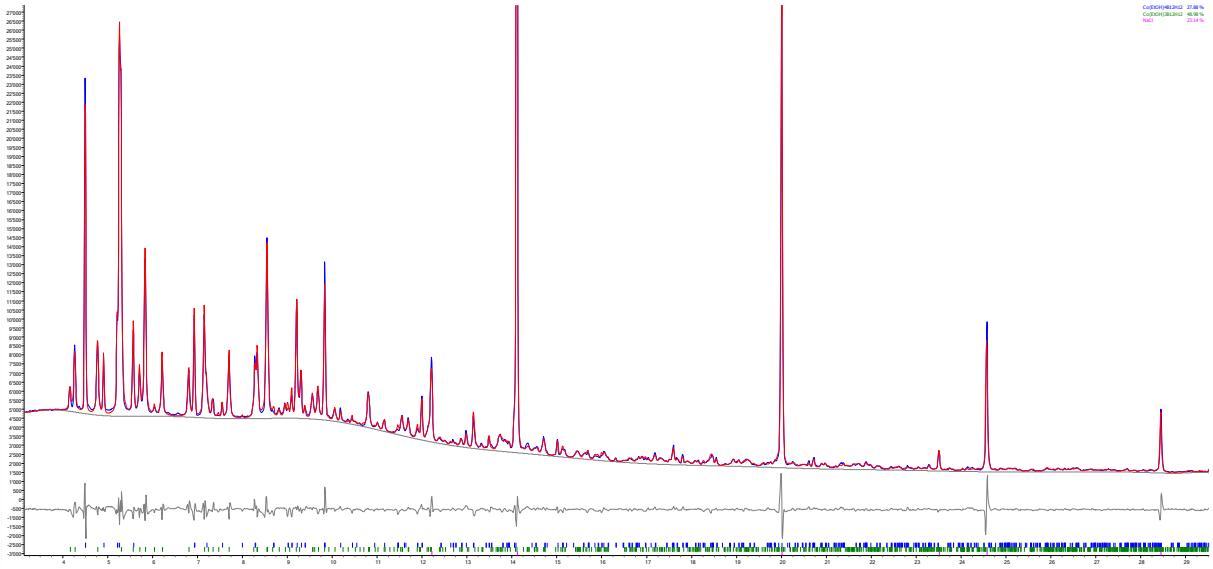

Figure S10. Rietveld plot for refinement of *m*-$Co(EtOH)_4B_{12}H_{12}$ at T= 69 °C. SNBL, λ= 0.69425 Å, χ^2 = 7278, R_{wp} (bgr. corrected) = 0.11, R_{Bragg} = 0.01.

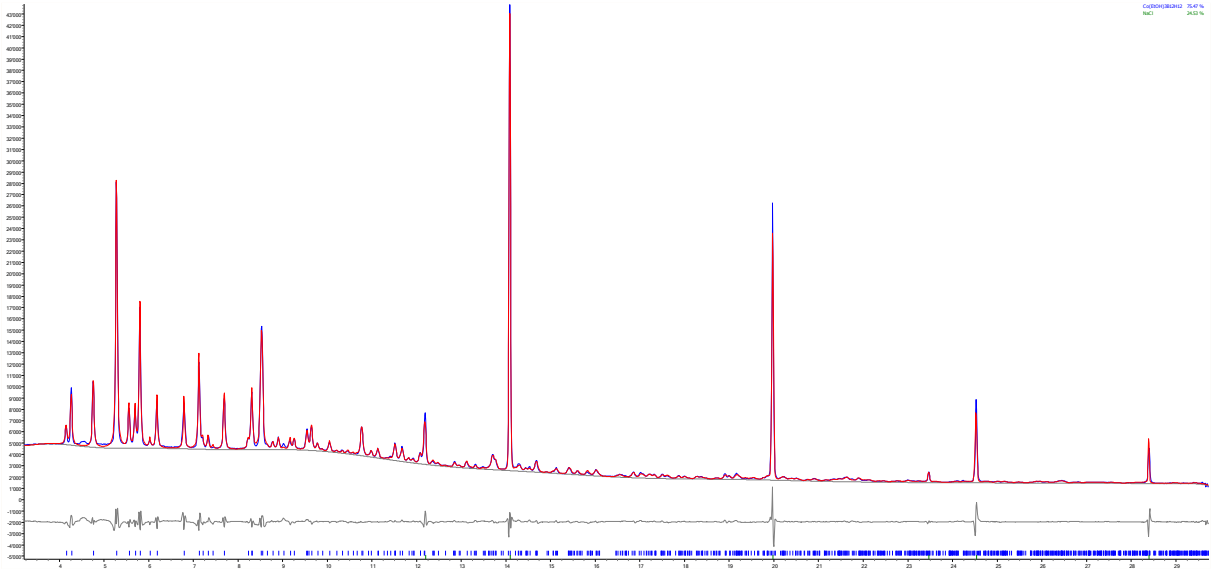

Figure S11. Rietveld plot for refinement of *m*-$Co(EtOH)_3B_{12}H_{12}$ at T= 108 °C. SNBL, λ= 0.69425 Å, χ^2 = 7506, R_{wp} (bgr. corrected) = 0.12, R_{Bragg} = 0.01.

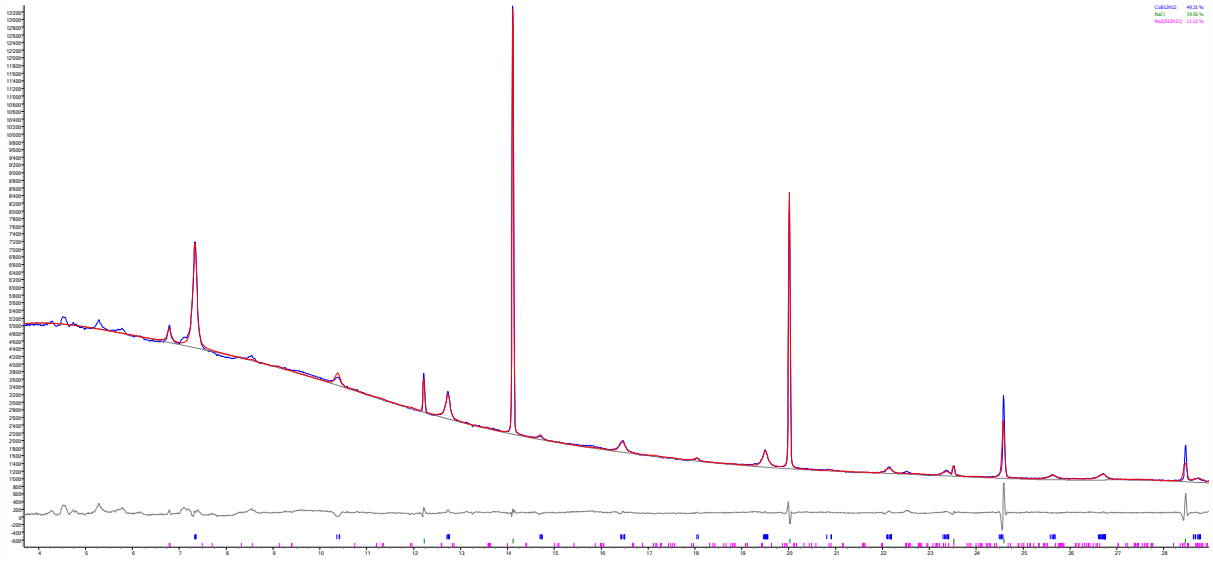

Figure S12. Rietveld plot for refinement of *r*-$CoB_{12}H_{12}$ at T= 32 °C. SNBL, λ= 0.69425 Å, χ^2 = 3213, R_{wp} (bgr. corrected) = 0.14, R_{Bragg} = 0.04.

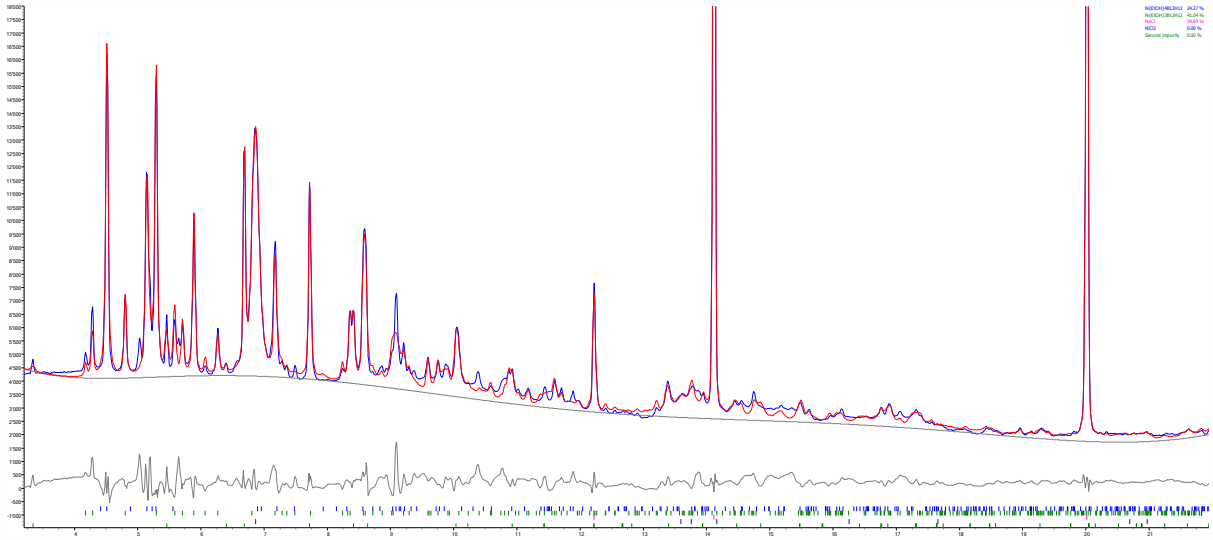

Figure S13. Rietveld plot for refinement of *m*-$Ni(EtOH)_4B_{12}H_{12}$ at T= 63 °C. SNBL, λ= 0.69425 Å, χ^2 = 12139, R_{wp} (bgr. corrected) = 0.13, R_{Bragg} = 0.02.

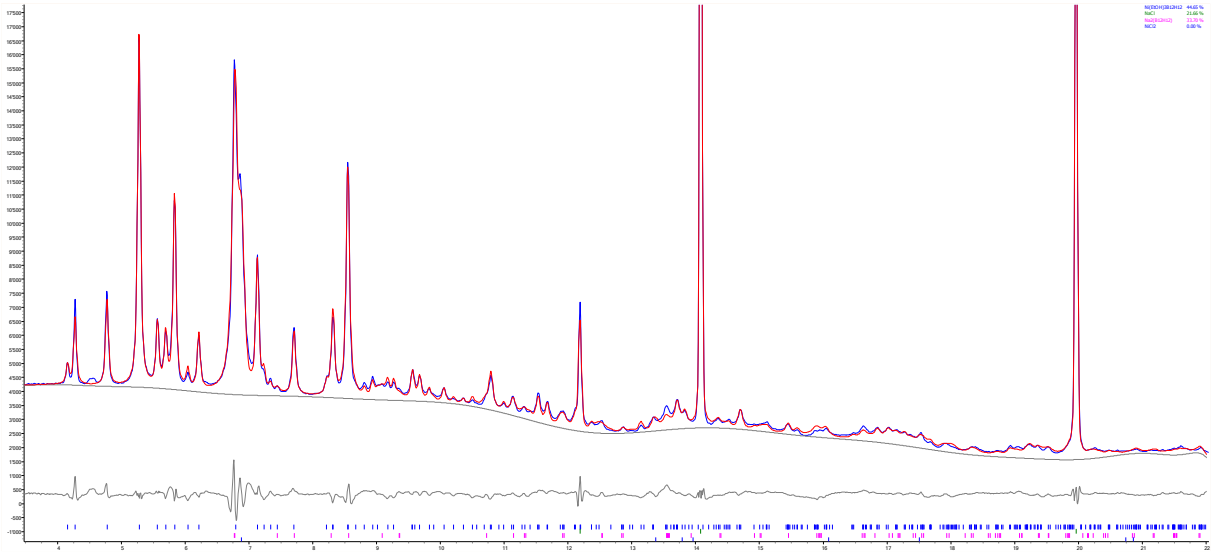

Figure S14. Rietveld plot for refinement of *m*-$Ni(EtOH)_3B_{12}H_{12}$ at T= 124 °C. SNBL, λ= 0.69425 Å, χ^2 = 6621, R_{wp} (bgr. corrected) = 0.08, R_{Bragg} = 0.01.

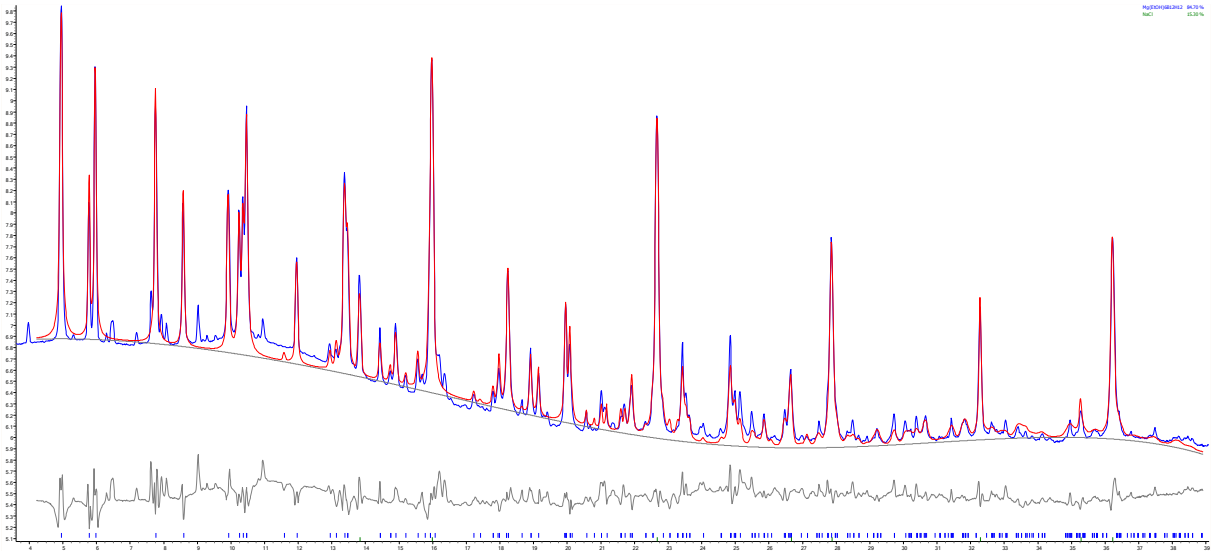

Figure S15. Rietveld plot for refinement of *tg*-$Mg(EtOH)_6B_{12}H_{12}$ at T= 30 °C. SNBL, λ= 0.7849 Å, χ^2 = 2074, R_{wp} (bgr. corrected) = 0.17, R_{Bragg} = 0.04.

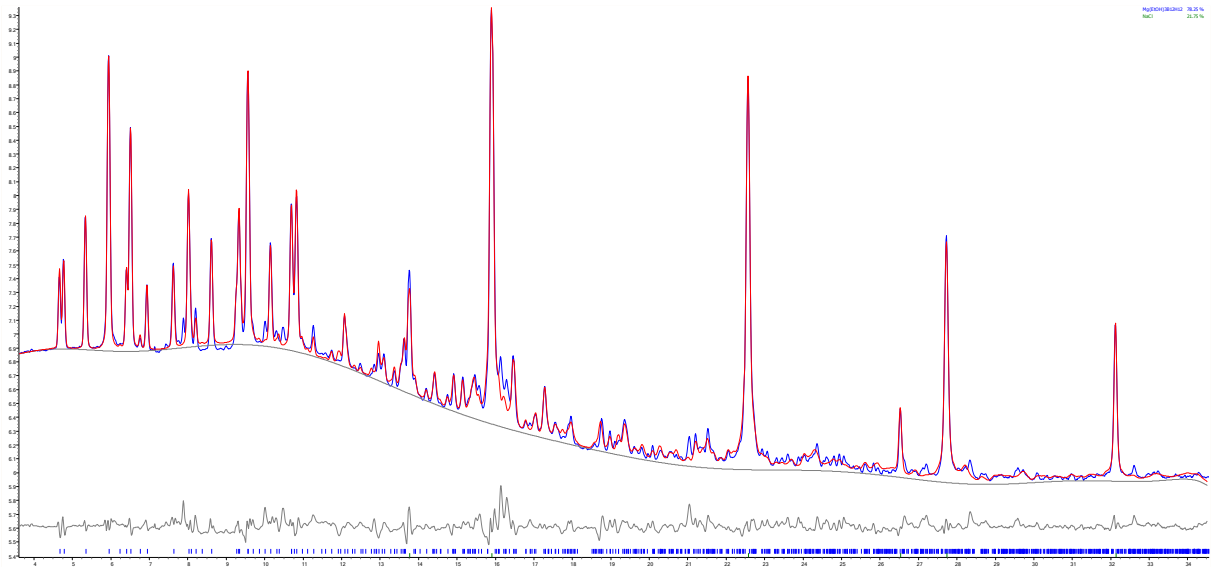

Figure S16. Rietveld plot for refinement of *m*-$Mg(EtOH)_3B_{12}H_{12}$ at T= 143 °C. SNBL, λ= 0.7849 Å, χ^2 = 712, R_{wp} (bgr. corrected) = 0.11, R_{Bragg} = 0.01.

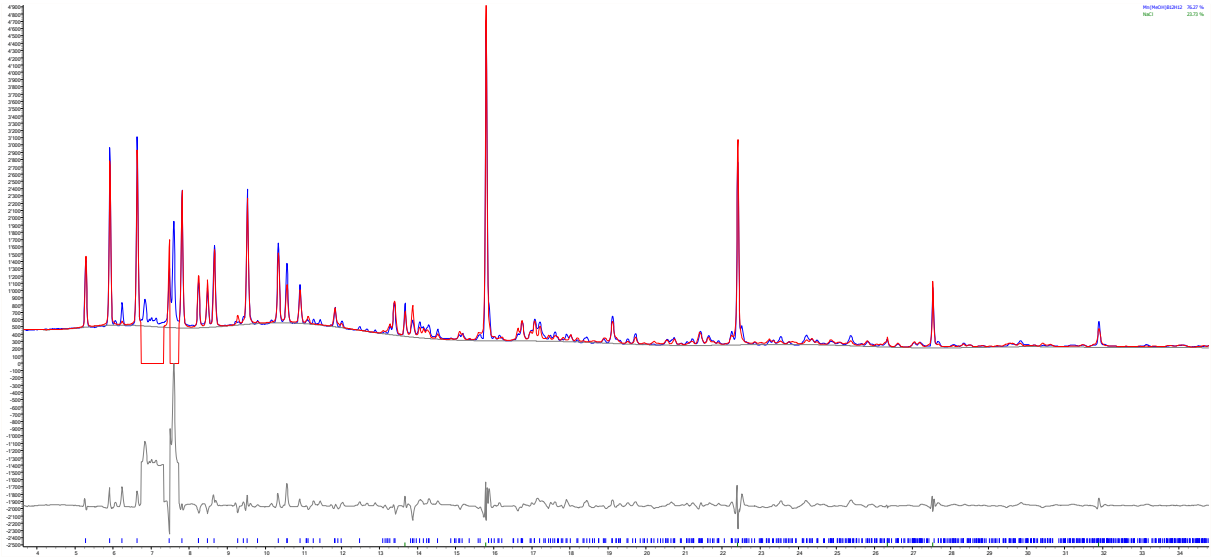

Figure S17. Rietveld plot for refinement of *o*-$Mn(MeOH)B_{12}H_{12}$ at T= 218 °C. SNBL, λ= 0.77936 Å, χ^2 = 1578, R_{wp} (bgr. corrected) = 0.23, R_{Bragg} = 0.06.

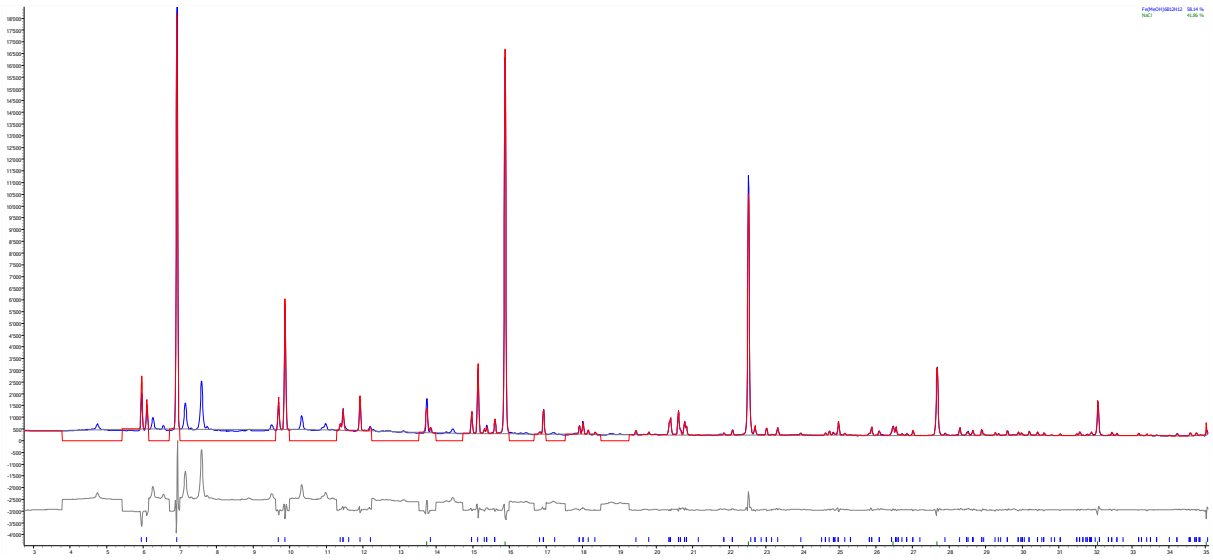

Figure S18. Rietveld plot for refinement of *r*-$Fe(MeOH)_6B_{12}H_{12}$ at T= 52 °C. SNBL, λ= 0.77936 Å, χ^2 = 2116, R_{wp} (bgr. corrected) = 0.13, R_{Bragg} = 0.04.

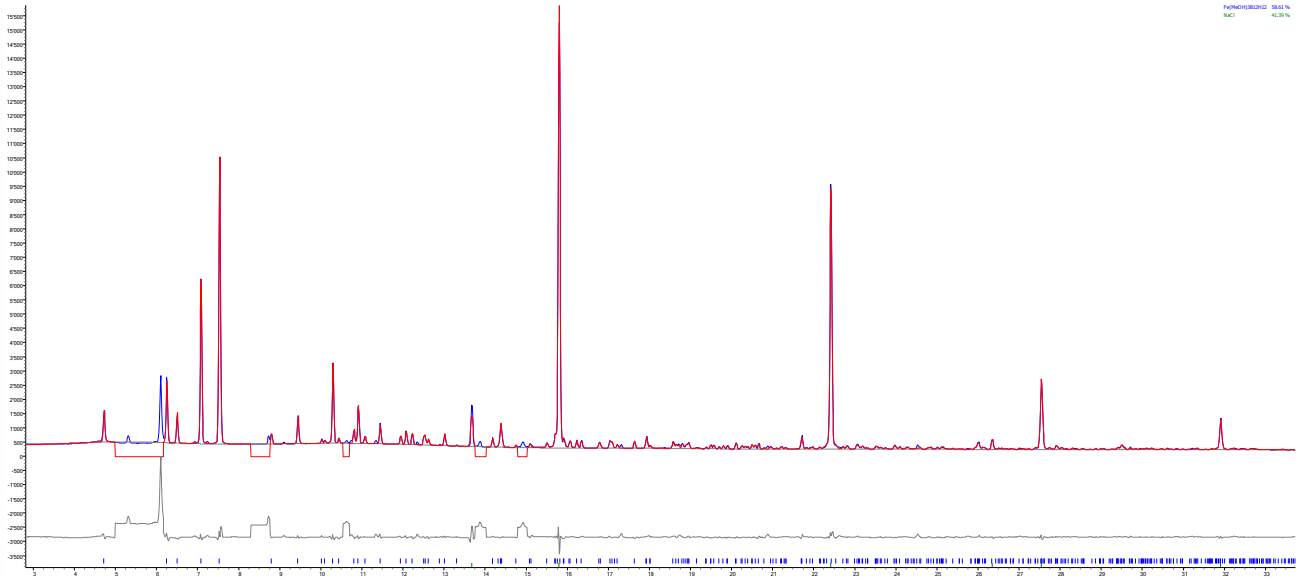

Figure S19. Rietveld plot for refinement of *m*-$Fe(MeOH)_3B_{12}H_{12}$ at T= 190 °C. SNBL, λ= 0.77936 Å, χ^2 = 829, R_{wp} (bgr. corrected) = 0.10, R_{Bragg} = 0.02.

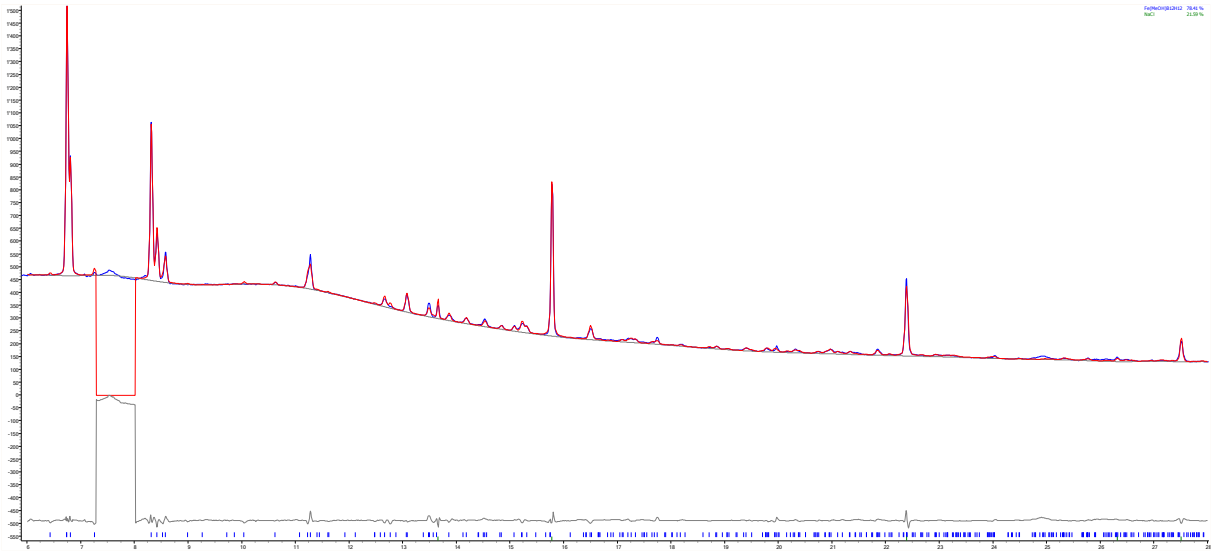

Figure S20. Rietveld plot for refinement of *m*-Fe(MeOH)$B_{12}H_{12}$ at T= 213 °C. SNBL, λ= 0.77936 Å, χ^2 = 43, R_{wp} (bgr. corrected) = 0.11, R_{Bragg} = 0.01.

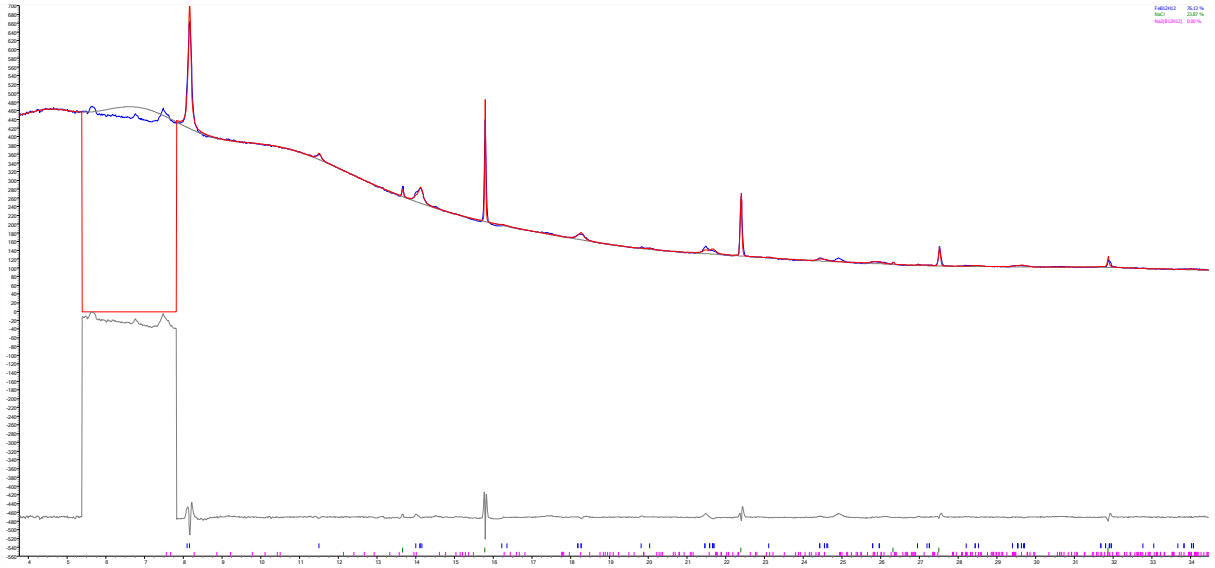

Figure S21. Rietveld plot for refinement of *r*-$FeB_{12}H_{12}$ at T= 217 °C. SNBL, λ= 0.77936 Å, χ^2 = 39, R_{wp} (bgr. corrected) = 0.26, R_{Bragg} = 0.01.

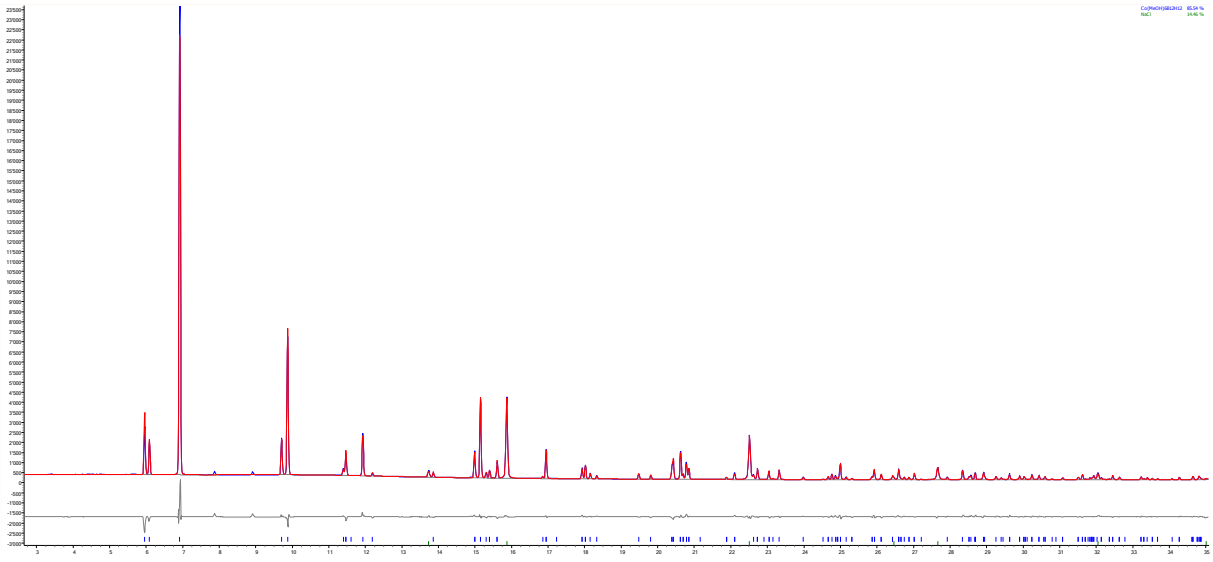

Figure S22. Rietveld plot for refinement of *r*-$Co(MeOH)_6B_{12}H_{12}$ at T= 62 °C. SNBL, λ= 0.77936 Å, χ^2 = 665, R_{wp} (bgr. corrected) = 0.10, R_{Bragg} = 0.04.

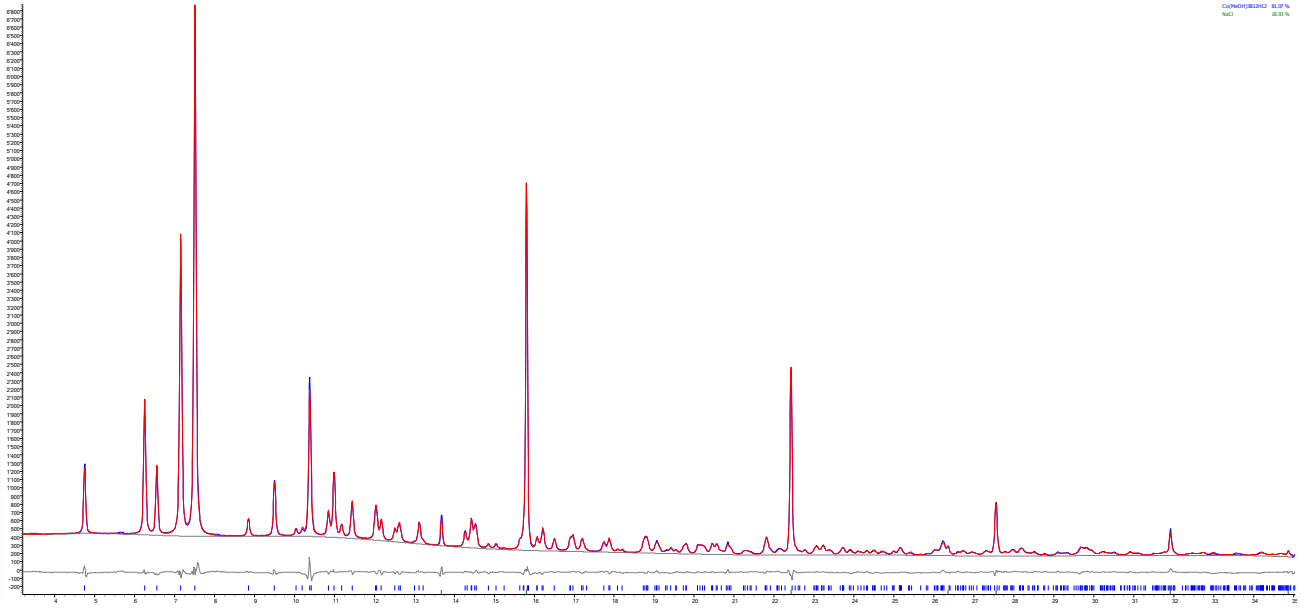

Figure S23. Rietveld plot for refinement of *m*-$Co(MeOH)_3B_{12}H_{12}$ at T= 190 °C. SNBL, λ= 0.77936 Å, χ^2 = 156, R_{wp} (bgr. corrected) = 0.06, R_{Bragg} = 0.01.

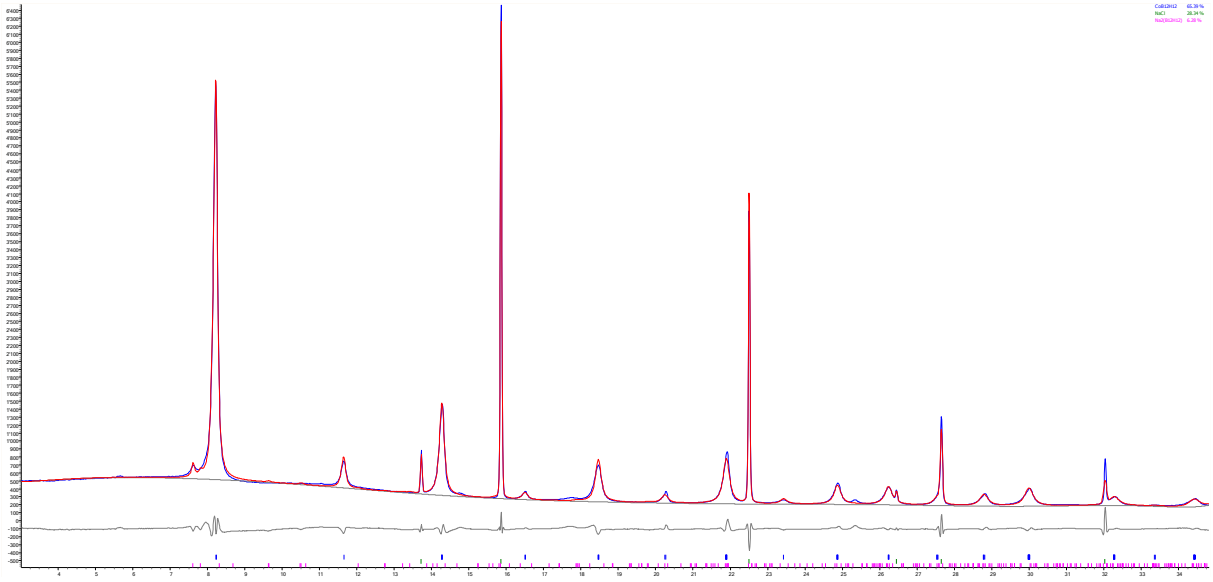

Figure S24. Rietveld plot for refinement of *r*-$CoB_{12}H_{12}$ at T= 65 °C. SNBL, λ= 0.77936 Å, χ^2 = 475, R_{wp} (bgr. corrected) = 0.10, R_{Bragg} = 0.01.

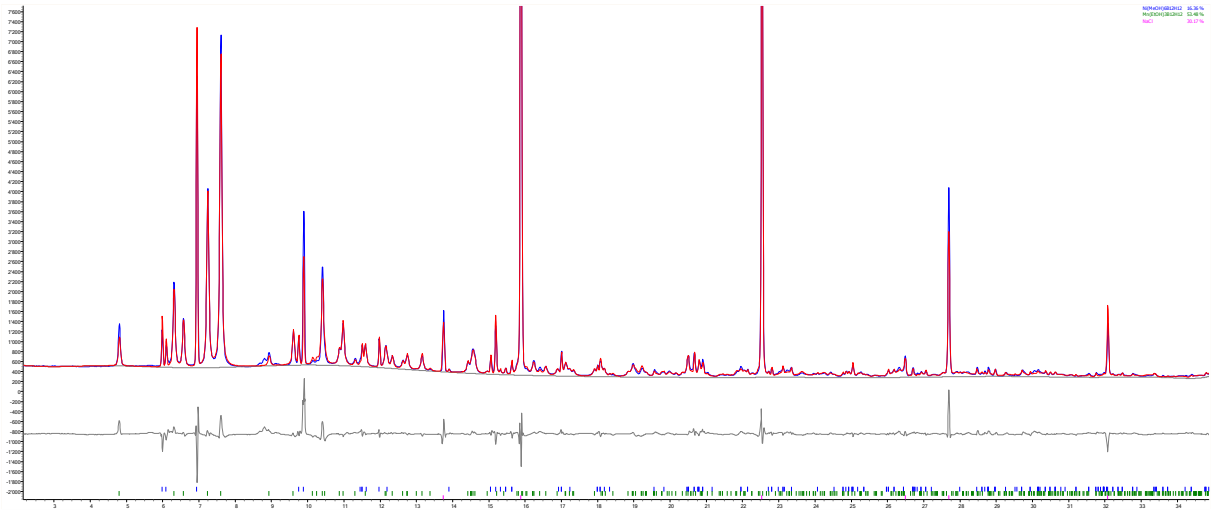

Figure S25. Rietveld plot for refinement of *r*-$Ni(MeOH)_6B_{12}H_{12}$ at T= 55 °C. SNBL, λ= 0.77936 Å, χ^2 = 1600, R_{wp} (bgr. corrected) = 0.13, R_{Bragg} = 0.08.

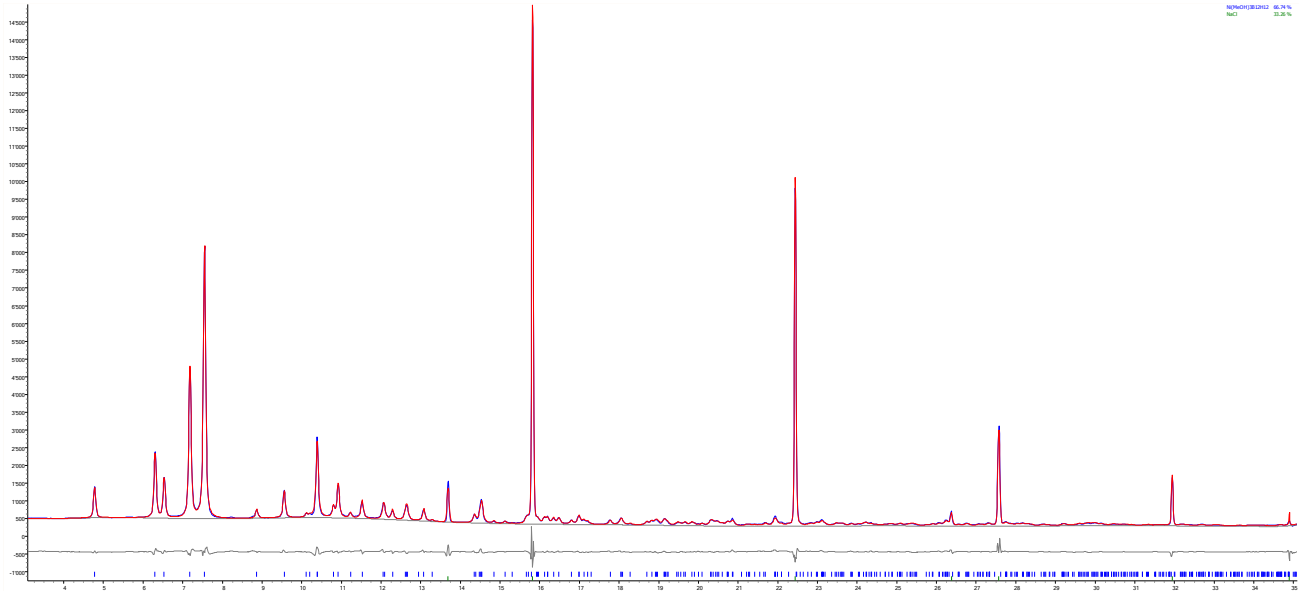

Figure S26. Rietveld plot for refinement of *m*-Ni(MeOH)$_3$B$_{12}$H$_{12}$ at T= 190 °C. SNBL, λ= 0.77936 Å, χ^2 = 458, R_{wp} (bgr. corrected) = 0.08, R_{Bragg} = 0.01.

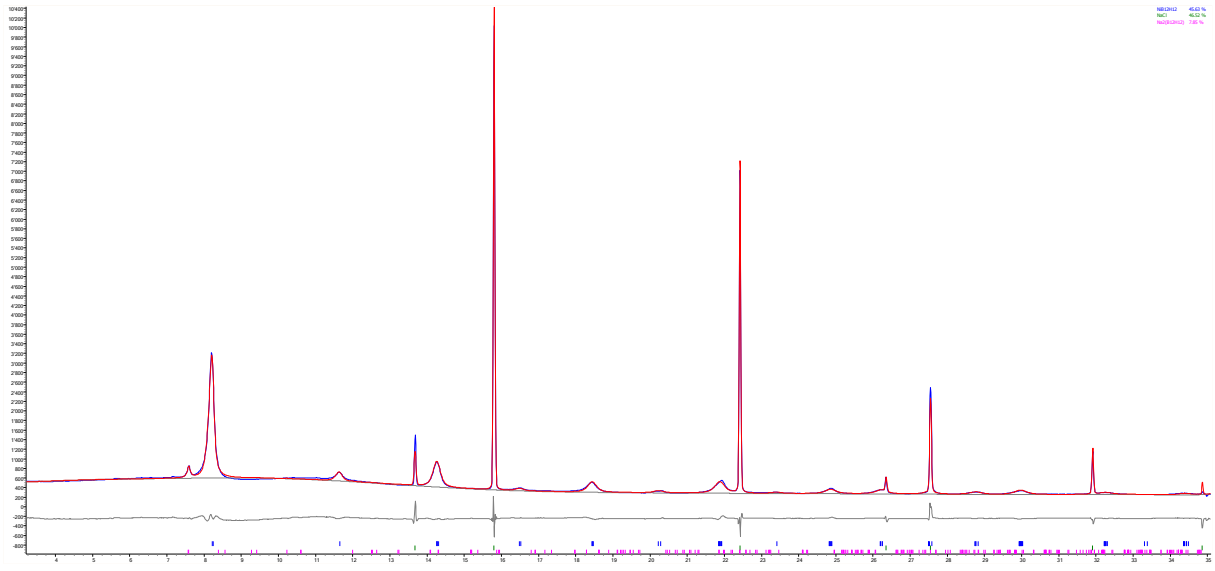

Figure S27. Rietveld plot for refinement of *r*-NiB$_{12}$H$_{12}$ at T= 225 °C. SNBL, λ= 0.77936 Å, χ^2 = 392, R_{wp} (bgr. corrected) = 0.10, R_{Bragg} = 0.01.

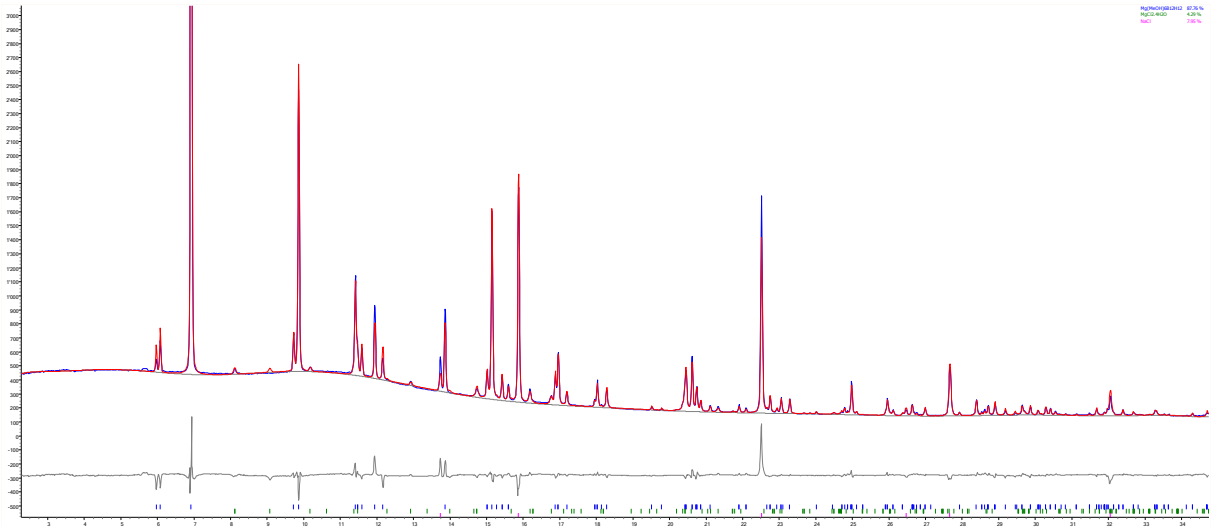

Figure S28. Rietveld plot for refinement of *r*-$Mg(MeOH)_6B_{12}H_{12}$ at T= 60 °C. SNBL, λ= 0.77936 Å, χ^2 = 320, R_{wp} (bgr. corrected) = 0.13, R_{Bragg} = 0.02.

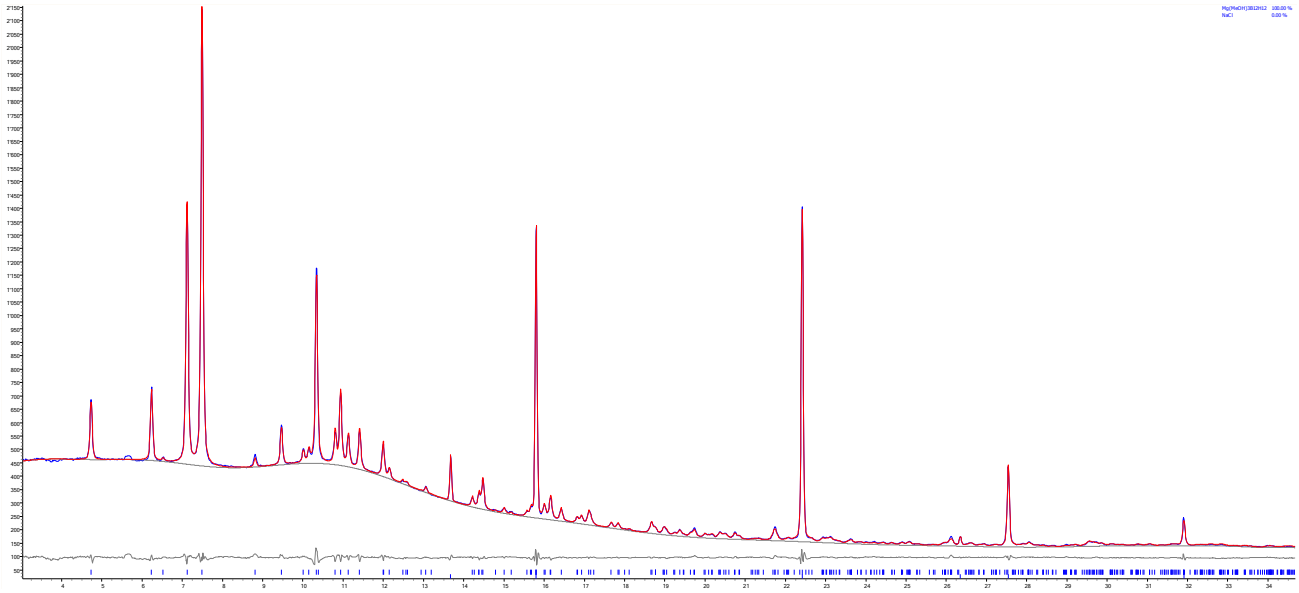

Figure S29. Rietveld plot for refinement of *m*-$Mg(MeOH)_3B_{12}H_{12}$ at T= 220 °C. SNBL, λ= 0.77936 Å, χ^2 = 21, R_{wp} (bgr. corrected) = 0.05, R_{Bragg} = 0.005.

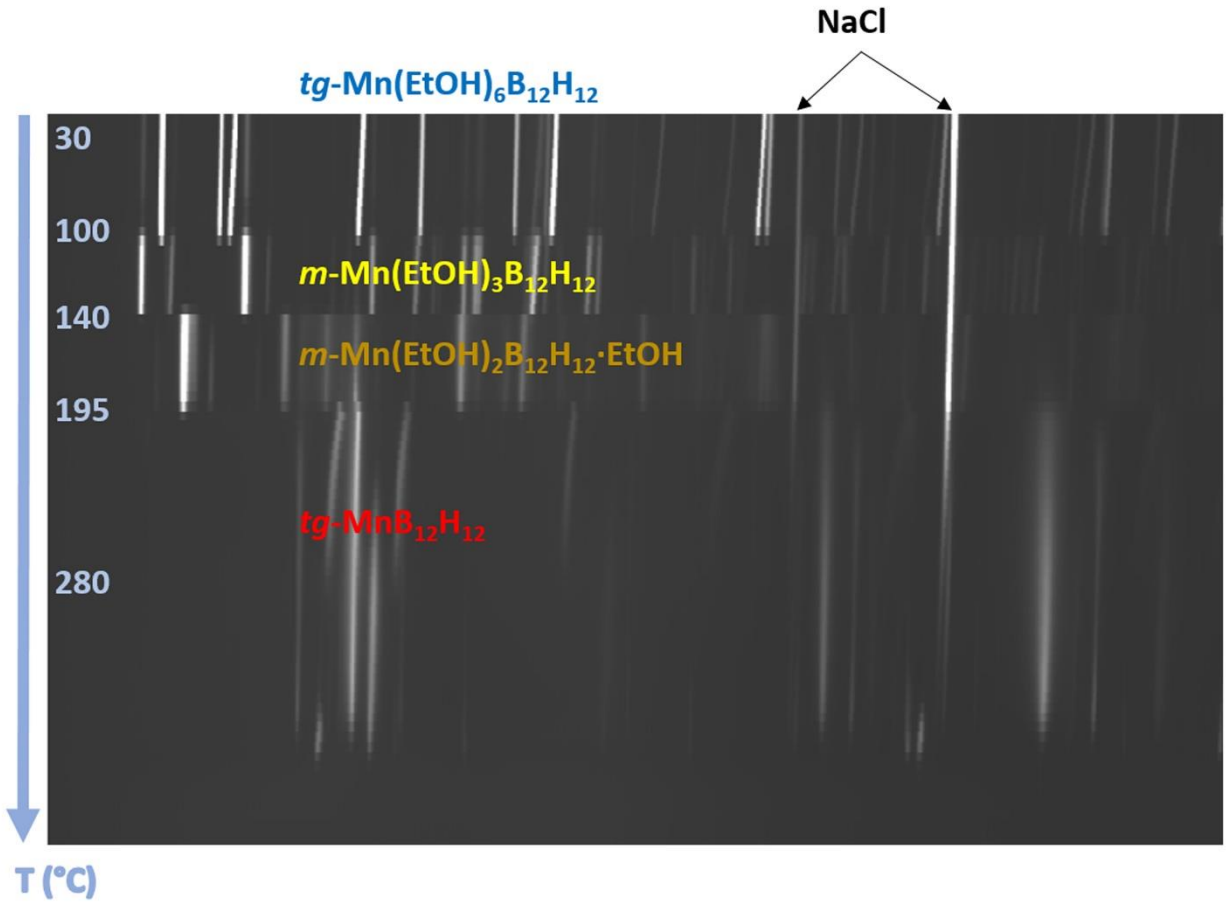

Figure S30. Temperature dependent X-ray powder diffraction patterns (T-ramp) for ball-milled $Na_2B_{12}H_{12}$ + $MnCl_2$ mixture loaded with ethanol (heating rate 10 K/min under dynamic vacuum, λ = 0.7225 Å).

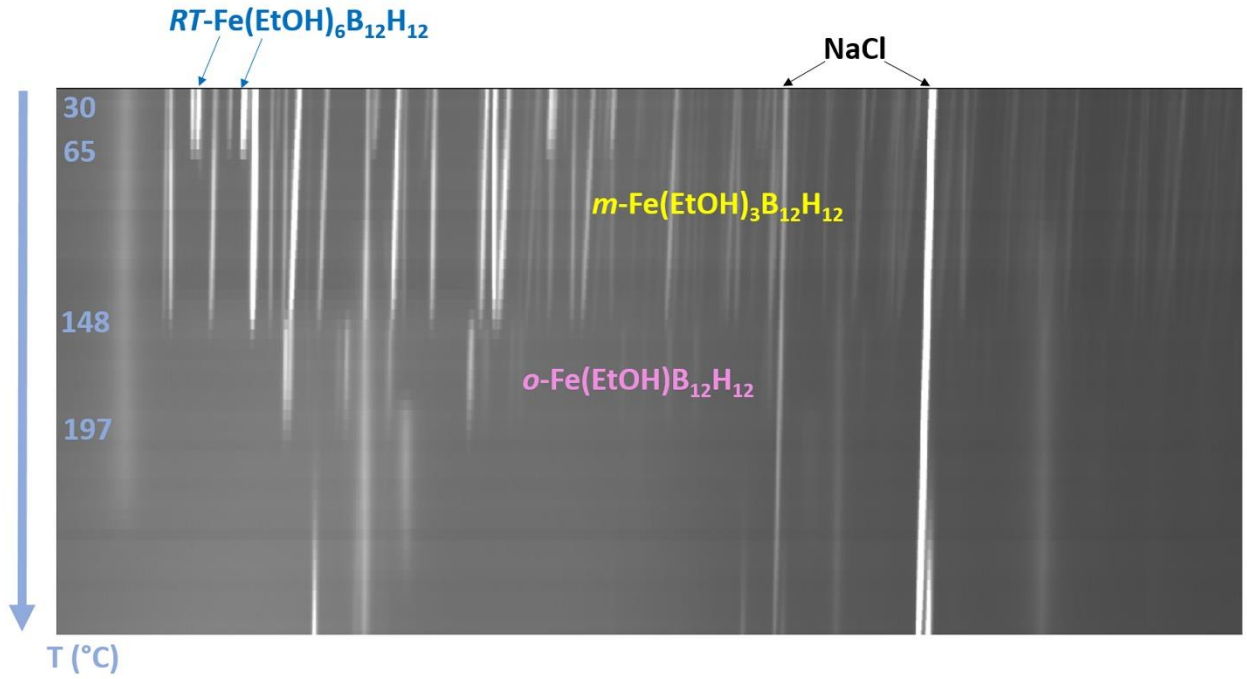

Figure S31. Temperature dependent X-ray powder diffraction patterns (T-ramp) for ball-milled $Na_2B_{12}H_{12}$ + $FeCl_2$ mixture with addition of ethanol (heating rate 10 K/min under dynamic vacuum, λ = 0. 7849 Å).

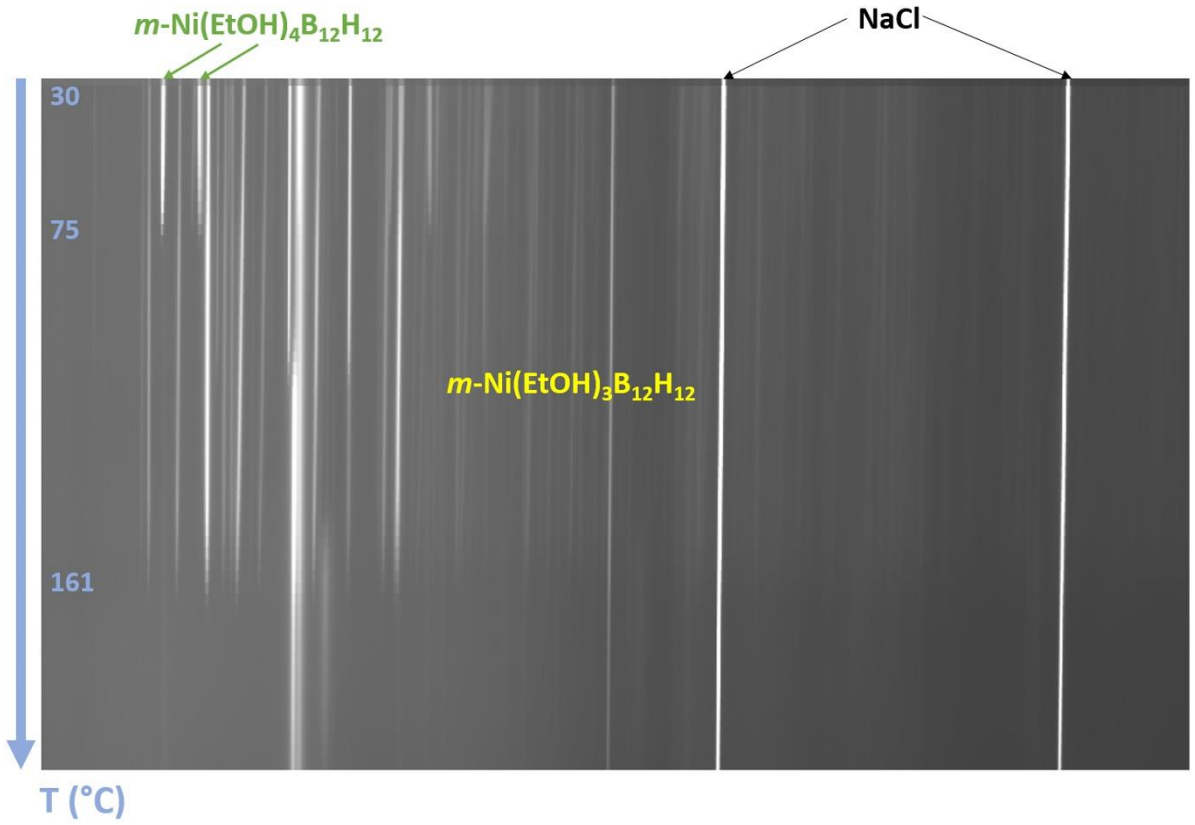

Figure S32. Temperature dependent X-ray powder diffraction patterns (T-ramp) for ball-milled $Na_2B_{12}H_{12}$ + $NiCl_2$ mixture with addition of ethanol (heating rate 10 K/min under dynamic vacuum, λ = 0. 69425 Å).

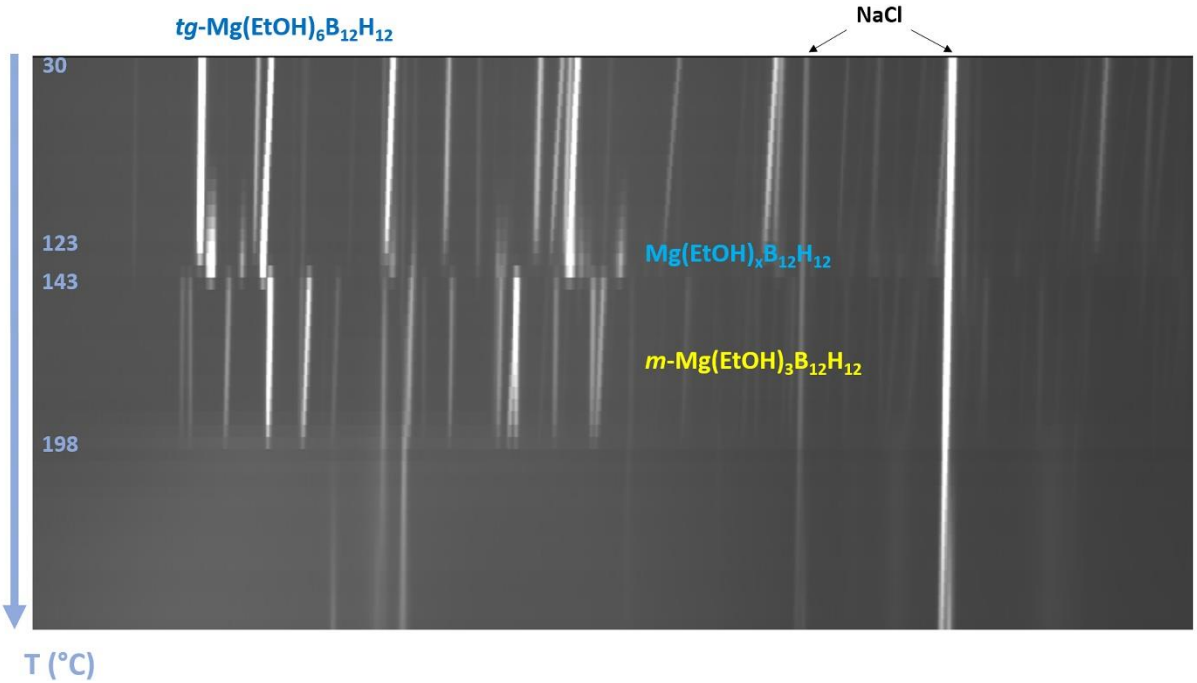

Figure S33. Temperature dependent X-ray powder diffraction patterns (T-ramp) for ball-milled $Na_2B_{12}H_{12}$ + $MgCl_2$ mixture with addition of ethanol (heating rate 10 K/min under dynamic vacuum, λ = 0. 7849 Å).

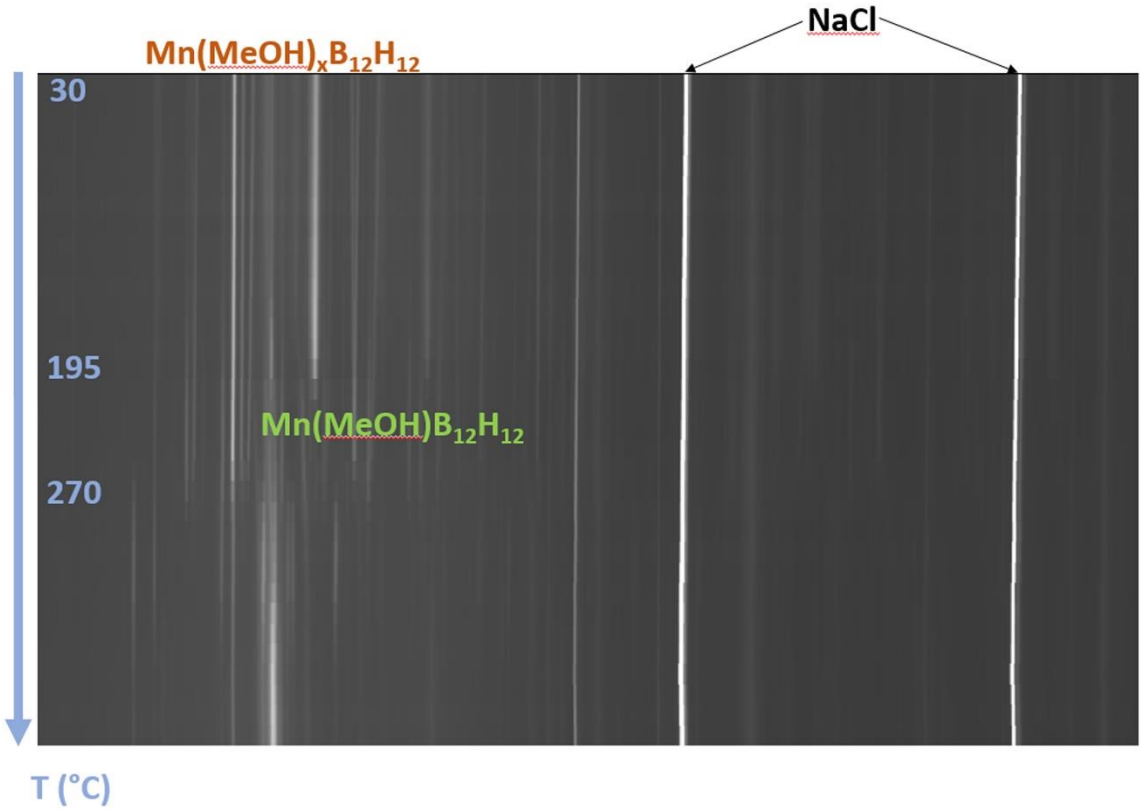

Figure S34. Temperature dependent X-ray powder diffraction patterns (T-ramp) for ball-milled $Na_2B_{12}H_{12}$ + $MnCl_2$ mixture loaded with ethanol (heating rate 10 K/min under dynamic vacuum, λ = 0.7225 Å).

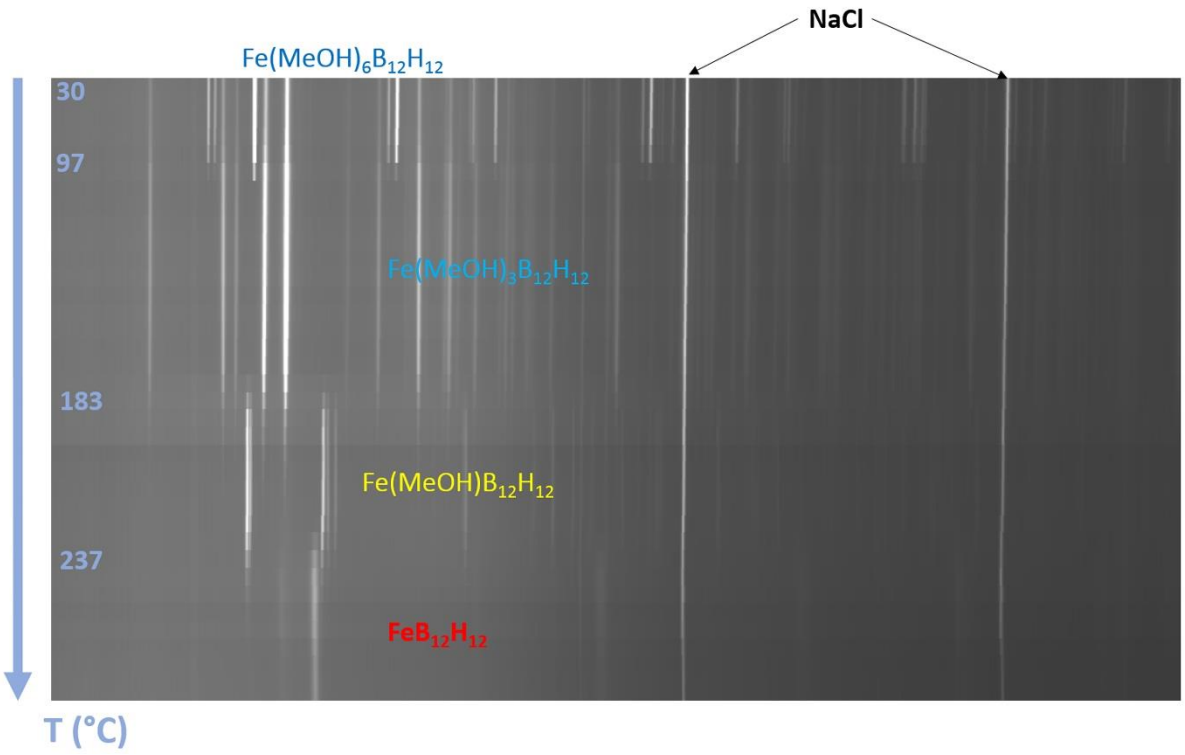

Figure 35. Temperature dependent X-ray powder diffraction patterns (T-ramp) for ball-milled $Na_2B_{12}H_{12}$ + $FeCl_2$ mixture with addition of methanol (heating rate 10 K/min under dynamic vacuum, λ = 0. 77936 Å).

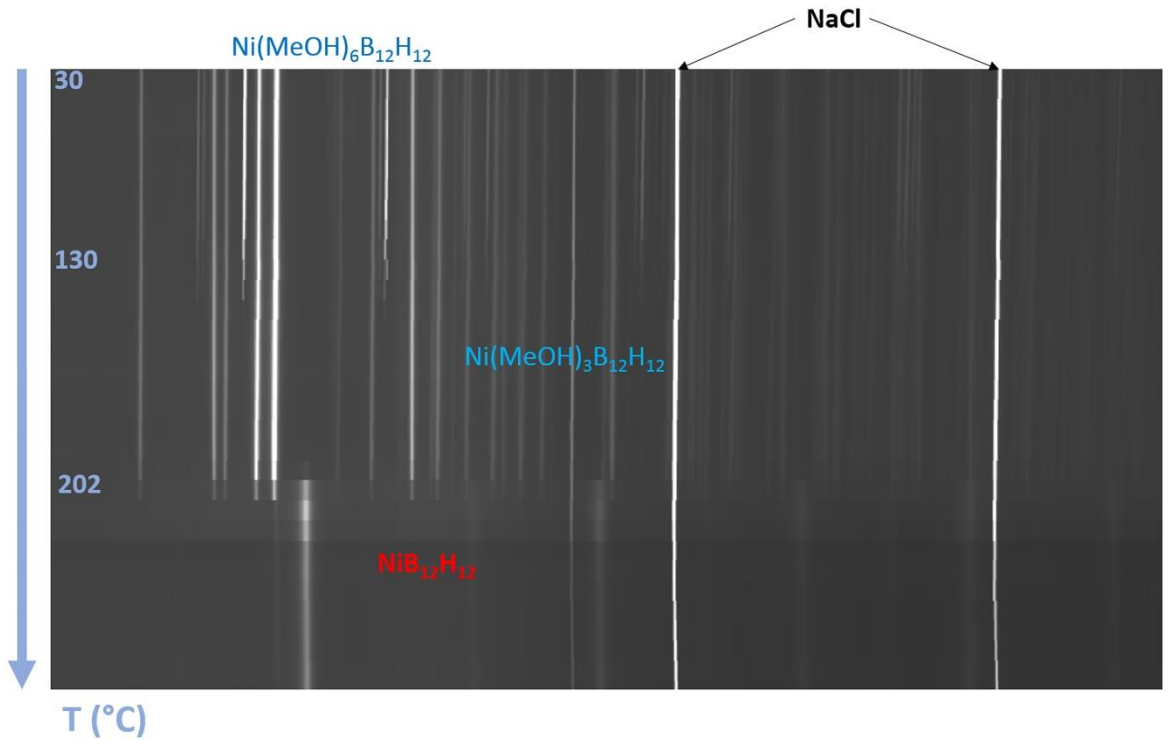

Figure 36. Temperature dependent X-ray powder diffraction patterns (T-ramp) for ball-milled $Na_2B_{12}H_{12}$ + $NiCl_2$ mixture with addition of methanol (heating rate 10 K/min under dynamic vacuum, λ = 0. 77936 Å).

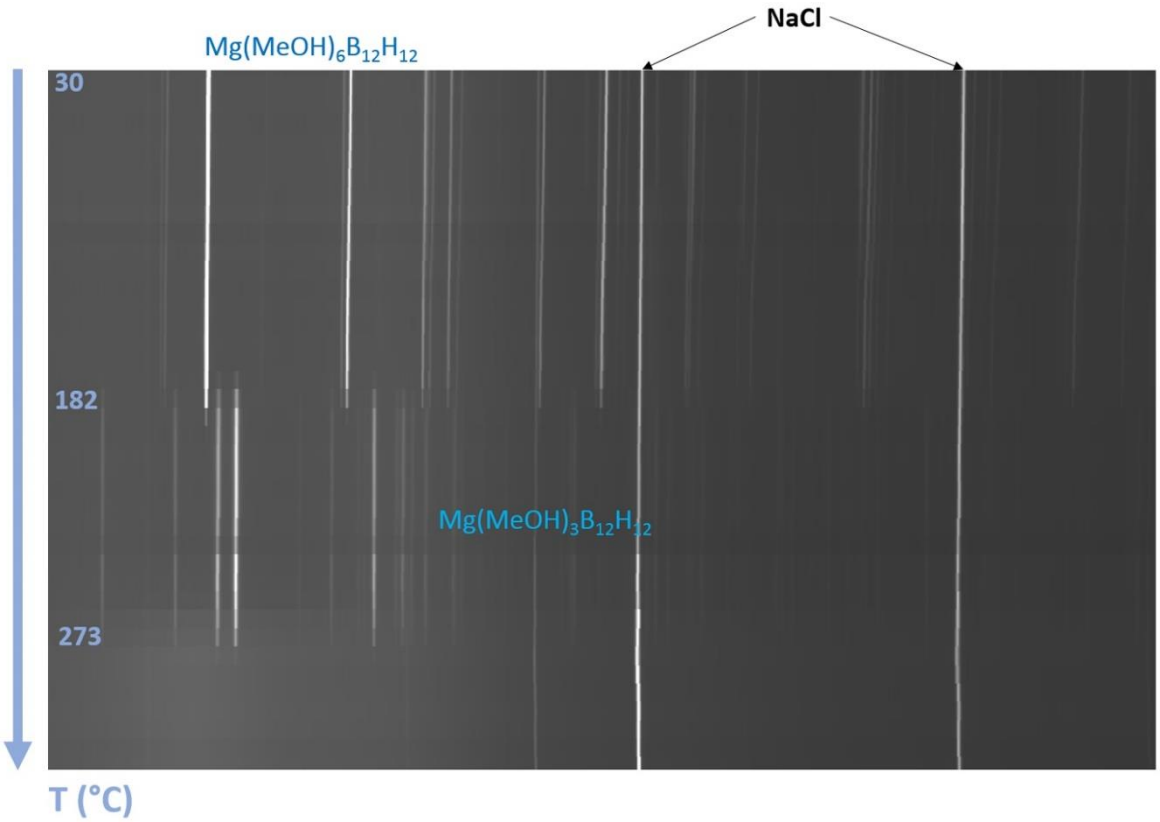

Figure 37. Temperature dependent X-ray powder diffraction patterns (T-ramp) for ball-milled $Na_2B_{12}H_{12}$ + $MgCl_2$ mixture with addition of methanol (heating rate 10 K/min under dynamic vacuum, λ = 0. 77936 Å).